DOI: 10.1002/ejic.200500950

Reactivity of Polyiodides Towards 1,3-Bis(4-pyridyl)propane (bpp): A New CuI Cluster Polycatenane Framework and a Novel 2D AgI Cluster Motif

Yunyin Niu,[a] Yinglin Song,[b] Ning Zhang,[a] Hongwei Hou*[a] Deji Che,[a] Yaoting Fan,[a] Yu Zhu,[a] and Chunying Duan[c]

Keywords: Clusters / Copper / Iodine / Lead / Organic–inorganic hybrid composites / Silver

The solution-phase reactions of metal iodides or iodine with 1,3-bis(4-pyridyl)propane (bpp) yields four new organic–inorganic hybrid frameworks, namely $[(CuI)_4(bpp)_4]_n$ (**1**), $[(AgI)_6(bpp)]_n$ (**2**), $[PbI_2(bpp)]_n$ (**3**), and $[I_3(bppH)]$ (**4**), each of which adopts a different structural motif. For example, complex **1** is a 2D "open" coordination polymeric cluster consisting of a CuI_2Cu rhomboid cluster core coordinated by *anti-anti* and *anti-gauche* bpp interactions to produce an interpenetrating 2D (4,4) polycatenane net; **2** is a novel bpp inclusion compound with a unique 2D polymeric hexagonal prism-shaped $[Ag_6I_6]_n$ cluster motif; compound **3** is also a 2D "open" supramolecular cluster made from $[PbI_2]_n$ "ribbons" and bpp bridges; compound **4** is a triiodide made up of organic $[bppH]^+$ cations and a I_3^- anion chain. The clusters **1**–**3** obtained from the reaction between polyiodide complexes and an organic ligand suggest that this simple synthetic approach is likely to be applicable to the construction of polymeric clusters. The third-order NLO effects of **1** were studied by Z-scan techniques. The polymeric cluster exhibits good nonlinearities and the effective third-order NLO refractive index (n_2) value is 2.56×10^{-12} esu which is comparable to those of most cluster monomers and polymers.

Introduction

The construction of supramolecular polymeric networks has been of great interest in recent years, not only due to their intriguing architectures and topologies[1] but also for their potential properties as functional solid materials in catalysis,[2] optics,[3] and magnetism.[4] In addition to the main driving forces of metal–ligand coordination and hydrogen bonding, weak interactions and other subtle factors such as molecular entanglement[5] and halogen–halogen interactions[6] can also have a dramatic effect on the assembly of extended porous topologies. Polycatenation can be regarded as regularly repeated infinite versions of the closed molecular loops via a topological Hopf link − the whole catenated array has a higher dimensionality than the component motifs for a possible combination of interlocking or interweaving covalent, mechanical, and coordination bonds.[5c,7] Since no genuine example of an organic polycatenane has been characterized, a number of metal-based molecular rings have been used as building blocks for the construction of polycatenanes. According to Fujita,[8] transition-metal-directed self-assembly is a designable and highly efficient catenane synthesis pathway, and the configuration of the bridging ligands plays an important role in the self-assembly of metal-based catenanes.

Polyiodides are well-known for their ability to form a vast diversity of extended networks with unique conducting and optical properties.[9] Studies have shown that their structures and macroscopic physical properties can be understood through the level of halogen–halogen interactions between three fundamental building blocks: the Lewis acid acceptor I_2, and the Lewis base donors I^- or I_3^-, and "guest" building blocks (e.g. metal iodides). These building blocks can be catenated easily and a large variety of polyiodides can be synthesized. The synthesis methods can be described simply as the addition of iodine to an iodide in an appropriate reaction medium, such as I_3^-: $I_2(s) + I^-(aq) \rightarrow I_3^-(aq)$. Recently, the reaction between monovalent metal halides MI ($M = Cu^+$, Ag^+) and I^- attracted our attention because the solubility of MI increases in mixed solvents (such as THF/H_2O and CH_3CN/H_2O) upon addition of excess KI. This increase in solubility may be a consequence of the formation of a metal diiodide anion: $MI(s) + I^- \rightarrow MI_2^-$. More importantly, the active intermediate MI_2^- ion is a good iodine source for cluster construction, and its self-assembly reaction with rigid and flexible bispyridyl ligands is an effective route for the preparation of novel polymeric complexes containing iodine clusters. The systematic incorporation of a metal iodide and organic spacer-based molecular rings within polymeric cluster networks allows for the

[a] Department of Chemistry, Zhengzhou University, Henan 450052, P. R. China
E-mail: houhongw@zzu.edu.cn
Fax: +86-371-6776-1744
[b] Department of Applied Physics, Harbin Institute of Technology, Heilongjiang 150001, P. R. China
[c] State Key Laboratory of Coordination Chemistry, Coordination Chemistry Institute, Nanjing University, Nanjing 210093, P. R. China

modulation of their structural and physical properties. With this method we have previously obtained a 2D "open" polymer $[AgI(bpe)]_n$ [bpe = 1,2-bis(4-pyridyl)ethane][10] and a unique 1D coordination polymeric cluster $\{[AgI(inh)]_6(KI)\}_n$ with hexagonal cluster units centered by μ_6-I.[11]

Herein we use bpp as a bridging ligand due to its networking ability[12] and its variable configurations (*anti-anti*, *anti-gauche*, and *gauche-gauche*; Figure 1), and report the formation of four bpp-based compounds by self-assembly with polyiodide species (Scheme 1): **1**–**3** are cluster compounds and **4** is a triiodide. The good nonlinear optical effects of cluster **1** are also presented.

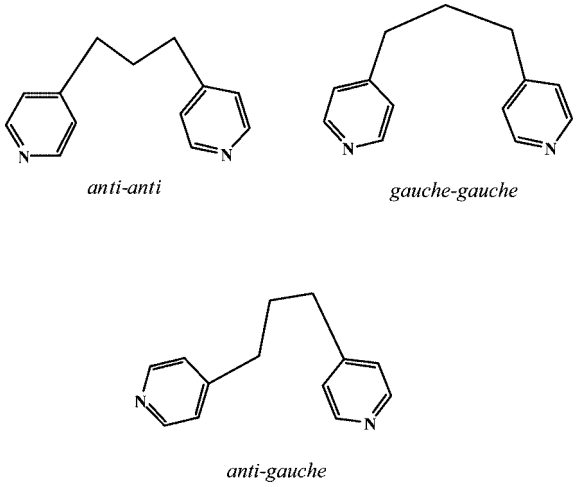

Figure 1. Three main coordination configurations of bpp.

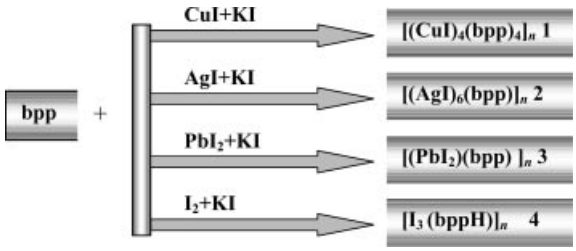

Scheme 1. Schematic view of the reactivity of polyiodides toward bpp under distinct conditions.

Results and Discussion

Preparation of Compounds

As far as the use of insoluble inorganic metal salts in coordination chemistry is concerned, their solubility is a crucial question to the related preparation procedure. Several strategies have been employed to circumvent this practical problem. Firstly, the use of an appropriate solvent. For example, THF is a superior solvent to dissolve HgI_2 as the solubility of HgI_2 in THF is about 20 times better than that in ethanol. More than ten HgI_2 coordination polymers have been obtained with the method.[13] The second procedure is solid-state reaction at low temperature. When an insoluble salt such as CuI or AgI is mixed and ground with Bu_4NBr (or Et_4NBr) and MoS_4^{2-}, the mixture reacts easily at room temperature or low temperature to give a soluble product in organic solvents. About six polymeric clusters with novel motifs have been synthesized with the method.[14] The third method involves finding a soluble precursor complex. When the concentration of X^- (X = Cl^-, Br^-, and I^-) increases to a certain level, the solubility of MX increases due to the formation of polyhalide anion complexes MX_2^-. This method has been used unintentionally by the addition of NaI, KI, HI, Bu_4NI, or Ph_4PI,[15] and moreover, we found a small quantity of water is helpful for accelerating the dissolution. Many insoluble metal iodides such as CuI, AgI, PbI_2, HgI_2, etc. can be dissolved efficiently by this method, and several interesting metal–iodine clusters have been found.[10,11] In this contribution, complex **1** was prepared as light-yellow crystals by the addition of a DMF solution of bpp to a THF/H_2O solution of CuI in excess KI. The product is insoluble in common organic solvents and stable in air.

Compound **2** was obtained by a similar procedure to that of **1**, except that the mixed solvent THF/CH_3CN/H_2O was used; the use of a single solvent (such as THF or CH_3CN) never gave a perfect crystal. Complex **2** was only obtained when the solvent evaporation was conducted in the dark and the solution was nearly dry.

For **3**, the dissolution of PbI_2 may obey the following well-known equation: $PbI_2 + 2KI \rightarrow K_2(PbI_4)$. Slow evaporation of the solution gives **3** as a colorless crystal. Compound **3** is also the first example of a PbI_2 coordination polymer obtained by the polyiodide reaction.

Compound **4** was obtained without a metal polyiodide. The formation of I_3^- shows its special stability in CH_3OH/H_2O.[9a] The N-protonation of bpp may be a result of protonation by the mixed solvents.

Crystal Structure of $[(CuI)_4(bpp)_4]_n$ (1)

In the structure of $[(CuI)_4(bpp)_4]_n$ (**1**), Cu^I adopts a distorted CuI_2N_2 tetrahedral coordination sphere and binds two pyridines from bpp and two bridging iodide counterions (Figure 2). Both the bridging iodides are also bound to another symmetry-related Cu^I center to form a $Cu(\mu_2\text{-}I)_2Cu$ rhombohedron. A similar unit is also present in dissociated dimeric molecules[16a,16b] and its self-assembly products with multitopic ligands.[16c–16j] Due to the flexibility of both the Cu–I–Cu and I–Cu–I angles, this CuI_2Cu rhomboid unit can adapt to a given coordination geometry produced by the ligands.[16b] In **1**, these metallic CuI_2Cu subunits connect alternately two couples of didentate bpp ligands to form a one-dimensional double-bridged polymeric chain which propagates along the *a* or *b* crystallographic direction. The doubly bridging iodides lie above and below the planes of the chain rings. An interesting feature of **1** is the parallelity of the CuI_2Cu metallacycles. All these cycles retain a plane perpendicular to the double-bridge surfaces, which shows that the bpp ligands have no evident impact on the CuI_2Cu configuration. On the other hand, the flexible

trimethylene spacer decreases the rigidity of the chain to cater for the parallelity of the CuI_2Cu rings. From this point of view, cluster **1** is a typical example of metal-directed self-assembly.

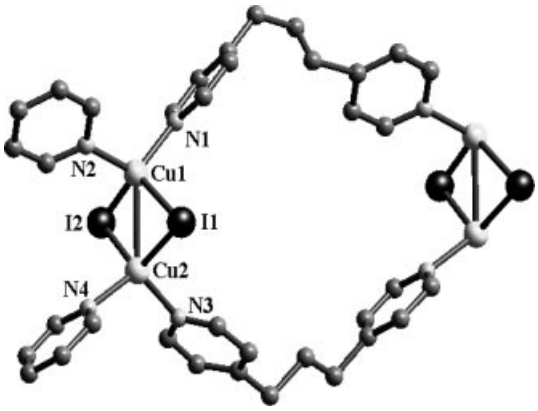

Figure 2. The elliptic molecular ring with approximate dimensions of 12.56×10.79 Å^2 in **1**.

Another noteworthy aspect of this structure is the existence of the interweaving linkages. In the doubly bridged chains, two such subunits and two bpp ligands with distinct conformations (*anti-anti* and *anti-gauche*) form an elliptic molecular ring with approximate dimensions of 12.56×10.79 Å^2. As mentioned above, there are two groups of equivalent chains extended along the *a* and *b* axes, respectively. Each closed elliptic circuit is penetrated by the same loop from another chain at the loosest point with a Hopf link (Figure 3, top), leaving no residual space for solvent inclusion. These two groups of interweaving chains display 2D "open" vertical interpenetration (Figure 3, bottom) to give a uniform (4,4) net containing square intermolecular boxes with approximate dimensions of 12.56×12.56 Å^2. The catenated coordination rings indicate an ideal separation between the ligands in each molecular ring, whereas catenation does not take place if the elliptical rings possess no voids in their cavities due to the possible excessive flexibility or the entanglement of the ligands. Compound **1** also emphasizes that optimized ligand conformations are essential for the self-assembly of catenanes.[8] Thus, this net is clearly different from other reported network topologies containing CuI_2Cu rhomboids[16g,16h] and represents the first uniform net of [2]-catenane nodes.

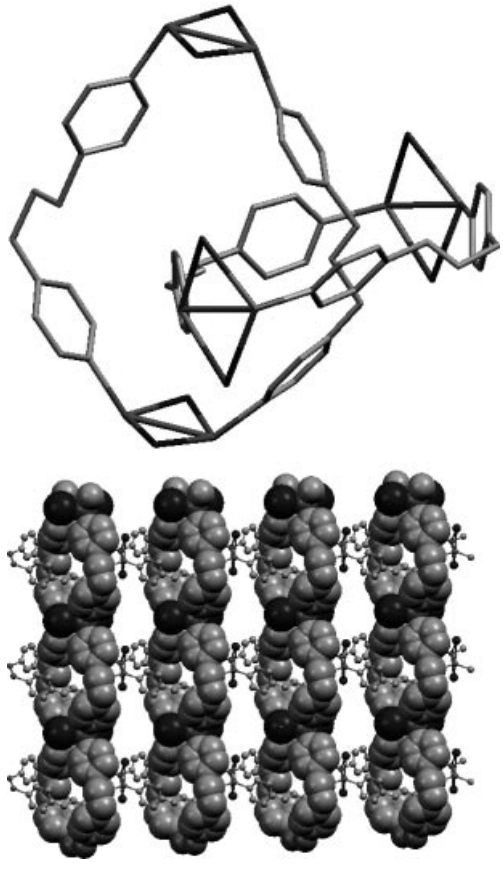

Figure 3. Solid-state structure of **1**. Top: The catenation of two individual $[(CuI)_2(bpp)_2]_n$ chains showing the Hopf links. Bottom: View along the *c*-direction the infinite interlocking 2D (4,4) lattice in **1** showing [2]-catenane nodes. The two individual polymeric chains are perpendicular to each other and are shown in capped-stick and space-filling representations, respectively.

Crystal Structure of $[(AgI)_6(bpp)]_n$ (2)

The X-ray single-crystal structural analysis showed that compound **2** crystallizes in the monoclinic system with space group *C*2/*c*. A portion of the cluster is shown in Figure 4. The structure of **2** is made up of isolated bpp units and the infinite polymeric cluster $[(AgI)_6]_n$.

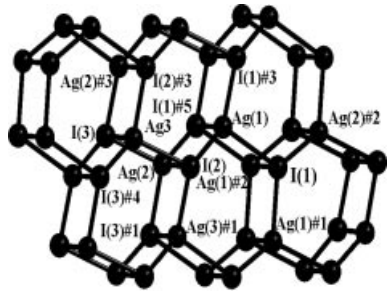

Figure 4. View of the two-dimensional $[AgI]_{6n}$ double layer in $[(AgI)_6(bpp)]_n$ (**2**).

In the polymeric structure, each silver atom is covalently bonded to three iodines at 2.77–2.87 Å in the same layer (Figure 4). The bond angles are in the range 102–114°. The iodine and silver atoms can therefore form six-membered rings but don't link up to form flat sheets. A fourth strong Ag–I covalent force with distances of 2.88–2.97 Å holds the layers together. This interaction prevents the layers from slipping over each other, which is different from the graphite lattice structure. The cluster can also be seen as a double layer (6,3) net motif composed of an edge-sharing Ag_6I_6 hexagonal prism-shaped cell. A section of the double layer of **2** is shown in Figure 5. There have been a series of polymeric metal(I) halide clusters reported;[17] comparing the crystallographic data available for different classes of silver

iodide clusters in the Cambridge Structural Database (CSD) and search results from the Chemical Abstracts database with SciFinder Scholar®, we see that compound **2** is the first example of a 2D bilayer AgI cluster motif.

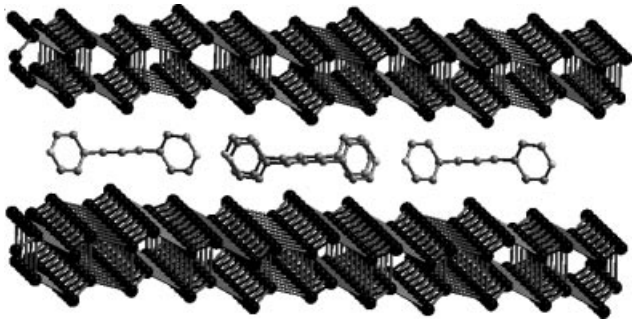

Figure 5. View showing the alternating $[AgI]_{6n}$ bilayer and bpp layer in **2**.

There is a closely related example for **2**, namely the triazine-based coordination polymer $[Cu_2I_2(tri)]_n$ (tri = triazine).[17b] In $[Cu_2I_2(tri)]_n$, the $[CuI]_n$ layer is also an undulating hexagonal net, with each six-membered ring adopting a boat conformation, but the fourth position of the tetrahedral copper center is occupied by a triazine nitrogen and triazine ligands link $[CuI]_n$ layers to give alternating copper(I) iodide and triazine layers. Because of the existence of bridging triazine layers, the longer distances between neighboring $[CuI]_n$ monolayers (minimum Cu–I distance is 6.2–7.1 Å) eliminate the possible Cu···I interlayer interactions. In **2**, the uncoordinated bpp is more like a cluster cutter and isolates the $[AgI]_n$ double layer unit from the metal polyiodide phase. The $[AgI]_n$ double layers are much more regular than $[CuI]_n$ in $[Cu_2I_2(tri)]_n$, so this structure can be considered to be a novel topological type for monovalent M^I halide polymeric clusters.

Crystal Structure of $[PbI_2(bpp)]_n$ (3)

An ORTEP drawing with the atom-numbering scheme of **3** is shown in Figure 6. The geometry around the lead atom is a distorted octahedron involving the nitrogen atom from pyridyl donors and the iodine atoms. Around the lead the four Pb–I distances range from 3.15 to 3.31 Å and the Ag–N distance is 2.64 Å. Each Pb also has a supramolecular interaction with a nitrogen atom from another bpp at a distance of 2.80 Å. The polymeric structure is comprised of $[PbI_2]_n$ "staircase clusters" and bpp bridges. The bpp ligands link cluster ribbons to form a 2D "open" motif spreading out in the *ab* plane. The bpp molecules stack along the *a*-axis with a stacking distance of 4.54 Å (to the neighboring equivalent pyridyl ring), forming a two-column structure between the $[PbI_2]_n$ ribbons. Each bpp ligand adopts an *anti-anti* configuration and the two pyridyl rings have a dihedral angle of 58.6°. The nearest Pb–Pb distance along the *a*-axis is equal to the repetition distance of bpp. The 2D sheets stack along the *c*-direction in an ABAB pattern, with the equivalent interlayer Pb–Pb separation distance being 11.92 Å. These 2D sheets are similar to those observed in $[PbX_2(4,4'\text{-bipy})]_n$,[18a] $[PbI_2(C_{12}H_{10}N_4)]_{2n}\cdot 0.5n(C_{12}H_{10}N_4)$,[18b] and $[PbI_2(L)]_n$ [L = *N*,*N*′-bis(3-pyridylmethyl)-1,4-biphenylenedimethyleneimine].[18c]

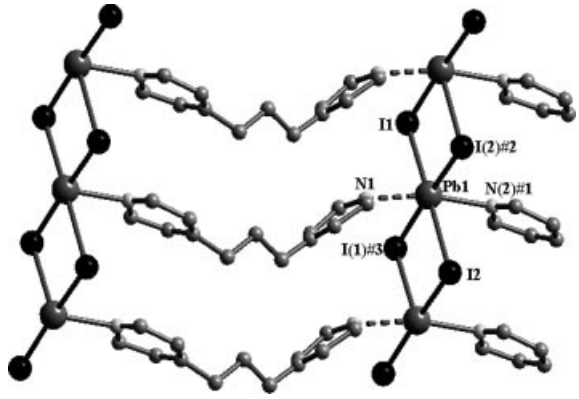

Figure 6. The 2D sheet structure of **3** formed by association of $[PbI_2]_n$ "staircase clusters" through supramolecular Pb···N interactions.

Crystal Structure of $[I_3(bppH)]$ (4)

The structure of **4** is made up of organic $[bppH]^+$ cations and I_3^- anion chains (Figure 7). The crystal packing is dominated by noncovalent donor–acceptor interactions involving both N–H···N (2.66 Å) hydrogen bonding between $bppH^+$ cations and I···I interactions between I_3^- anions. The triiodide ion is nearly linear (I2–I1–I3 = 178.12°) and asymmetric, and has *d*(I–I) distances of 2.901 and 2.921 Å. The triiodide ions are stacked in zigzag patterns with weak $I_3^-\cdots I_3^-$ interactions (3.69 Å). It is believed that the large linear deformation of the I_3^- ion is a result of the different environments in the solid state. Packing effects and electrostatic interactions may be considered to explain the induced asymmetry of I_3^- here.[9a] In **4**, all these interactions are considerably shorter than the sums of the van der Waals contact distances for the atoms involved (N: 1.55–1.61 Å; I: 1.98–2.00 Å).[19] The *anti-anti* configuration of bpp is also retained.

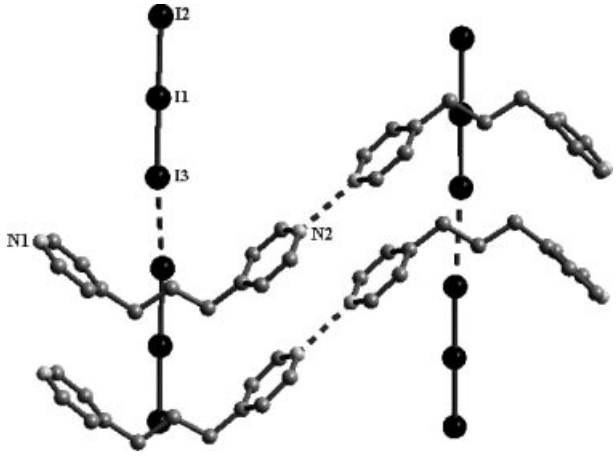

Figure 7. Crystal structure of polyiodide **4**.

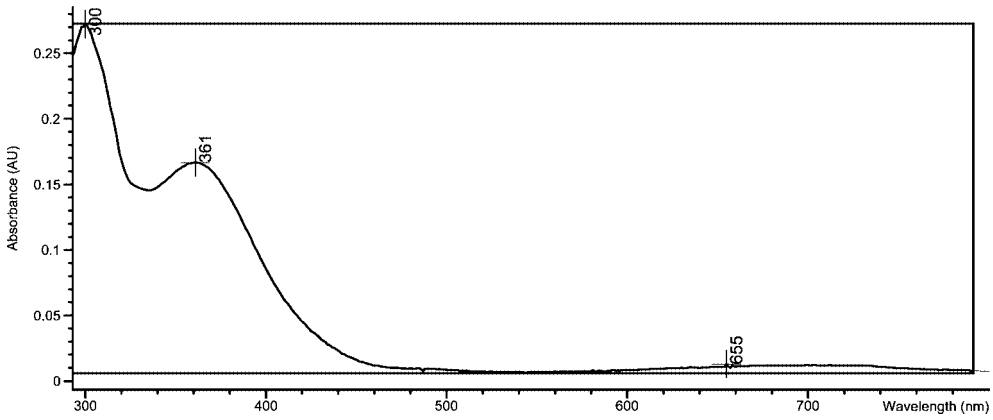

Figure 8. UV/Vis spectra of compound **1**.

Third-Order NLO Properties of 1

UV/Vis Spectra of 1

In the ground state UV/Vis spectra (Figure 8) of **1**, two strong absorption peaks at 300 and 361 nm in the near ultraviolet (UV) wavelength range are attributed to the charge-transfer excitation between Cu^+ and I^- ions of the cluster segment, perhaps the HOMO (mostly iodide in character) to LUMO (mostly metal) cluster-centered transition suggested by ab initio calculations.[20] In the visible region, there is a weak linear absorption at 655 nm assigned to d-d ligand field (LF) transition.[21]

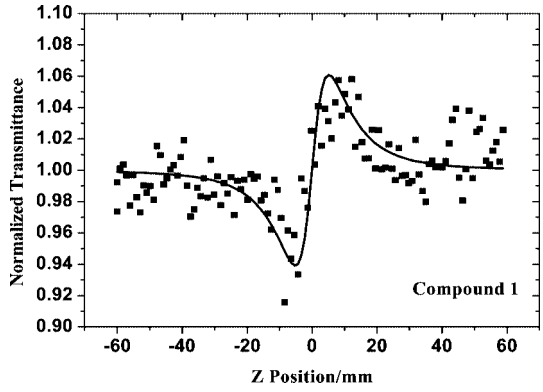

Figure 9. *Z*-scan measurement of the cluster **1** in 1.28×10^{-4} M DMF solution.

Nonlinear Effects of 1

A preliminary study of the third-order NLO properties of **1** was carried out by the *Z*-scan method in a 1.28×10^{-4} M DMF solution. The compound exhibits strong nonlinear optical behavior at 532 nm and the nonlinear optical properties are dominated by nonlinear refraction. The *Z*-scan data of the compound are given in Figure 9. The filled boxes are the experimental data measured under an open aperture. The nonlinear refractive components of the compound were assessed by dividing the normalized *Z*-scan data obtained in an open-aperture configuration. An effective third-order nonlinear refractive index, n_2, can be derived from the difference between normalized transmittance values at valley and peak positions (ΔT_{V-P}) by using Equation (1), where ΔT_{V-P} is the difference between normalized transmittance values at valley and peak positions, α_0 is the linear coefficient, L is the sample thickness, I is the peak irradiation intensity at focus, and λ is the wavelength of the laser. The effective third-order NLO refractive index was calculated to be 2.56×10^{-12} esu. The data show that the cluster has a positive sign for refractive nonlinearity, and the valley–peak pattern of the normalized transmitted curve obtained in the closed-aperture configuration shows the characteristic self-focusing behavior of propagating light in the sample.

$$n_2^{eff} = \frac{\lambda\alpha_0}{0.812\pi I\left(1-e^{-\alpha_0 L}\right)}\Delta T_{V-P} \quad (1)$$

Although this value of n_2 was obtained with a dilute solution of **1**, it is better than many best known third-order materials in neat solid form, such as SiO_2 (2×10^{-20} m^2W^{-1}) and CdS (2.5×10^{-18} m^2W^{-1}),[22] $SrLaGa_3O_7$ (11.1×10^{-20} m^2W^{-1}) and $Ca_2Ga_2SiO_7$ (6.5×10^{-20} m^2W^{-1}).[23] In particular, the n_2 value is also comparable to that of some clusters, including monomers, oligomers, and polymers in solution, such as the nest-shaped cluster $[MoOS_3Cu_3I(py)_5]$ (3.0×10^{-17} m^2W^{-1}),[24] the hexagonal prism cluster $[W_2S_8Ag_4(AsPh_3)_4]$ (5.9×10^{-17} m^2W^{-1}),[25] and the 2D microporous cluster $[MoS_4Cu_6I_4(py)_4]_n$ (2.5×10^{-17} m^2W^{-1}).[26] We speculate that the NLO properties of **1** are enhanced, in part, by the planar skeleton and the Cu^I–bpp molecular rings in the cluster. The heavy-atom effects of the planar "open" structures in **1** may allow better spin–orbital couplings, and thus intersystem crossing at the excited states.[27] In addition, the use of heavy atoms such as Cu and I may introduce more sublevels into the energy hierarchy and provide more allowed electronic transitions for the initial excited state in

1. The increased numbers of allowed electronic transitions probably enhance the nonlinear optics. On the other hand, these planar clusters have higher symmetry than other clusters. This higher symmetry, as in the phthalocyanine systems,[28] may decrease the probability of ground-state electronic transitions and gives a smaller absorption cross-section, σ_g, and a larger σ_e/σ_g (K_α) ratio. Our recent results have also shown that sometimes the metal core and peripheral ligands may have a complimentary effect on the strength of the NLO properties.[29] This presentation is the first report on the coordination chemistry of metallic polyiodides where the systematic incorporation of metal iodide and organic ligand-based molecular rings into polymeric cluster networks allows for the fine modulation of their structural and optical properties. In addition, although the concentration of coordination polymeric clusters in solution is apparently limited by their poor solubility, larger nonlinear index values may be expected if higher concentrations are attained.

Conclusions

The metal halides CuI, AgI, and PbI_2 form three different polymeric networks with bpp depending upon the coordination geometry of the metals and the reaction condition. In **2** bpp isn't coordinated to the Ag atoms, presumably due to the additional structural rigidity and stability of the 2D $(AgI)_n$ polymer sheet. The use of mixed organic solvents (THF/CH_3CN/H_2O) shows that the formation of **2** is also sensitive to the experimental conditions.[12d,12e] The choice of bpp as ligand is of great importance in determining the cluster skeleton (0D $[Cu_2I_2]$ for **1**, 1D $[PbI_2]_n$ for **3**, and 2D $[(AgI)_6]_n$ for **2**) and the final topology of the supramolecular arrays.

In summary, we have prepared and characterized the first uniform polycatenane (4,4) net with good NLO properties. The current work shows that this metallic polyiodides approach, which incorporates a metal-organic molecular ring or altering cluster skeletons into polymeric species, is perhaps a promising research direction in the search for better NLO materials. Further systematic investigation will focus on the influence of assembly conditions on the diversity of cluster networks and the design and construction of better NLO materials like the planar "open" coordination polymeric cluster **1**. Studies are under way to extend this facile method to other metal polyiodide anions, and to further probe their structure/properties relationship.

Experimental Section

Genaral: 1,3-Bis(4-pyridyl)propane (bpp) was obtained from Aldrich. Other chemicals were obtained from commercial sources and used as received. All solvents were pre-dried with activated molecular sieves and refluxed over the appropriate drying agents under argon. The IR spectrum was recorded with a Shimazu IR435 spectrometer as KBr disk (4000–400 cm^{-1}). UV/Vis spectra of **1** were measured with a HP 8453 ultraviolet-visible spectrophotometer. The C, H, and N microanalyses were performed with a Perkin–Elmer 240C instrument.

Preparation of $[(CuI)_4(bpp)_4]_n$ (1): A DMF solution of bpp (19.8 mg, 0.1 mmol) was added to a stirring colorless solution of CuI (19 mg, 0.1 mmol) dissolved in 10 mL of THF/H_2O (volume ratio of 1:5) in the presence of excess KI (99.6 mg, 0.6 mmol). The solution was then filtered and slowly evaporated in a vial at room temperature. Light-yellow crystals of **1** suitable for X-ray analysis were obtained after several days in about 22% yield. $C_{52}H_{56}Cu_4I_4N_8$ (1554.8): calcd. C 40.17, H 3.63, N 7.21; found C 40.36, H 3.70, N 7.20. IR (KBr): $\tilde{\nu}$ = 1608(vs), 1423 (s), 1218 (m), 809 (m) cm^{-1}. UV/Vis (DMF): λ_{max} ($\log\varepsilon$) = 300.0 nm (3.327), 361.0 (3.115), 655.0 (2.004).

Preparation of $[(AgI)_6(bpp)]_n$ (2): Compound **2** was obtained by a similar reaction procedure from bpp, AgI, and KI (molar ratio = 1:1:6) in THF/CH_3CN/H_2O at room temperature. Upon slow evaporation in the dark, colorless needles of **2** were harvested in 47% yield when the solution was nearly dry. $C_{13}H_{14}Ag_6I_6N_2$ (1606.9): calcd. C 9.74, H 0.88, N 1.75; found C 9.56, H 0.76, N 1.24. IR (KBr): $\tilde{\nu}$ = 3428 (sh), 3139 (sh), 2983 (w), 1710 (w), 1620 (s), 1400 (s), 1177 (w), 814 (w), 619 (w), 545 (w) cm^{-1}.

Preparation of $[PbI_2(bpp)]_n$ (3): Compound **3** was obtained by a similar reaction procedure from bpp, PbI_2, and KI (molar ratio = 1:1:2) in DMF/H_2O at room temperature. A colorless polymer **3** was harvested in 25% yield after 1 month. $C_{13}H_{14}I_2N_2Pb$ (659.25): calcd. C 23.64, H 2.14, N 4.24; found C 23.56, H 2.20, N 4.24. IR (KBr): $\tilde{\nu}$ = 2940 (w), 1606 (s), 1425 (w), 1221 (w), 1010 (m), 815 (m), 514 (w) cm^{-1}.

Preparation of $[I_3(bppH)]$ (4): Compound **4** was obtained by a similar reaction procedure from bpp, I_2, and KI (molar ratio = 1:1:2) in CH_3OH/H_2O at room temperature. Needle-shaped, dark-red crystals of **4** were obtained in 32% yield after 1 d. $C_{13}H_{15}I_3N_2$ (579.97): calcd. C 26.92, H 2.61, N 4.83; found C 26.86, H 2.56, N

Table 1. Selected bond lengths [Å] and angles [°] for **1**.[a]

Cu1–N2	2.048(6)	Cu1–N1#1	2.067(6)	Cu1–I1	2.6521(12)
Cu2–I1	2.6031(11)	Cu2–N3#1	2.058(6)	Cu1–I2	2.6690(11)
Cu2–I2	2.6756(11)	Cu2–N4	2.061(7)	N1–Cu1#2	2.067(6)
N2–Cu1–N1#1	113.3(2)	N2–Cu1–I1	104.22(17)	N1–Cu1–I1	109.55(17)
N2–Cu1–Cu2	112.85(19)	N1#1–Cu1–Cu2	133.88(16)	N1#1–Cu1–I2	107.16(17)
I1–Cu1–Cu2	57.50(3)	I2–Cu1–Cu2	59.06(3)	N2–Cu1–I2	106.8(2)
N4–Cu2–I1	111.4(2)	N3#1–Cu2–I2	104.21(18)	I1–Cu1–I2	115.96(4)
N4–Cu2–I2	106.2(2)	N3#1–Cu2–N4	108.4(3)	N3#1–Cu2–I1	108.73(19)
Cu2–I1–Cu1	63.28(3)	I1–Cu2–I2	117.44(4)	N3#1–Cu2–Cu1	130.71(17)
N4–Cu2–Cu1	120.64(19)	Cu1–I2–Cu2	62.11(3)	I1–Cu2–Cu1	59.23(3)
I2–Cu2–Cu1	58.83(3)	C5–N1–Cu1#2	122.4(5)	C1–N1–Cu1#2	120.8(5)

[a] Symmetry transformations used to generate equivalent atoms: #1: $x + 1, y, z$; #2: $x - 1, y, z$.

Table 2. Selected bond lengths [Å] and angles [°] for **2**.[a]

Ag(1)–I(1)	2.853(3)	Ag(1)–I(2)	2.860(3)	Ag(1)–I(1)#5	2.891(3)	Ag(1)–I(1)#3	2.841(3)
I(1)–Ag(1)#1	2.841(3)	I(1)–Ag(1)#2	2.891(3)	Ag(2)–I(2)	2.971(4)	Ag(2)–I(3)	2.770(3)
Ag(2)–I(3)#1	2.782(3)	Ag(2)–I(1)#5	2.870(4)	I(1)–Ag(2)#2	2.870(4)	I(2)–Ag(3)	2.839(3)
I(3)–Ag(2)#3	2.782(3)	Ag(3)–I(3)#4	2.821(3)	Ag(3)–I(2)#3	2.867(3)	I(3)–Ag(3)	2.888(3)
I(2)–Ag(3)#1	2.867(3)	I(3)–Ag(3)#4	2.821(3)				
Ag(1)#1–I(1)–Ag(1)	106.49(11)	Ag(1)#1–I(1)–Ag(2)#2	106.68(10)	Ag(1)–I(1)–Ag(2)#2	113.43(10)	Ag(1)#1–I(1)–Ag(1)#2	72.88(8)
Ag(1)–I(1)–Ag(1)#2	72.70(8)	Ag(2)#2–I(1)–Ag(1)#2	64.70(11)	Ag(3)–I(2)–Ag(1)	98.43(9)	Ag(3)–I(2)–Ag(3)#1	106.17(10)
Ag(1)–I(2)–Ag(3)#1	104.59(9)	Ag(1)–I(2)–Ag(2)	63.80(10)	Ag(3)–I(2)–Ag(2)	65.35(9)	Ag(2)–I(3)–Ag(2)#3	110.49(13)
Ag(2)#3–I(3)–Ag(3)	67.22(10)	Ag(3)#1–I(2)–Ag(2)	65.04(9)	Ag(2)–I(3)–Ag(3)	67.34(10)	Ag(2)–I(3)–Ag(3)#4	115.38(11)
Ag(2)#3–I(3)–Ag(3)#4	102.44(10)	Ag(3)#4–I(3)–Ag(3)	77.48(10)	I(1)#3–Ag(1)–I(1)	106.49(11)	I(1)#3–Ag(1)–I(2)	112.37(10)
I(1)#3–Ag(1)–Ag(2)	130.65(11)	I(2)–Ag(1)–I(1)#5	117.17(11)	I(1)–Ag(1)–I(2)	105.77(9)	I(1)#3–Ag(1)–I(1)#5	107.37(9)
I(2)–Ag(1)–Ag(2)	59.86(10)	I(1)#5–Ag(1)–Ag(2)	57.31(10)	I(1)–Ag(1)–I(1)#5	107.05(9)	I(3)#1–Ag(2)–I(1)#5	105.09(12)
I(3)–Ag(2)–I(3)#1	110.49(13)	I(3)–Ag(2)–I(1)#5	98.41(11)	I(1)–Ag(1)–Ag(2)	122.73(10)	I(3)#1–Ag(2)–I(2)	113.85(11)
I(3)–Ag(2)–I(2)	113.38(11)	I(3)#1–Ag(2)–Ag(1)	127.79(13)	I(1)#5–Ag(2)–Ag(1)	57.99(9)	I(3)–Ag(2)–Ag(1)	120.28(11)
I(1)#5–Ag(2)–Ag(3)	122.49(12)	I(2)–Ag(2)–Ag(1)	56.34(10)	I(3)–Ag(2)–Ag(3)	58.13(8)	I(2)#3–Ag(3)–I(3)	113.84(10)
I(1)#5–Ag(2)–Ag(3)#1	129.68(13)	I(3)#1–Ag(2)–Ag(3)	131.71(15)	I(1)#5–Ag(2)–I(2)	114.33(12)	I(2)–Ag(3)–Ag(2)	59.37(9)
I(2)–Ag(2)–Ag(3)#1	55.87(9)	I(2)–Ag(2)–Ag(3)	55.29(9)	I(3)–Ag(2)–Ag(3)#1	131.66(15)	I(3)#4–Ag(3)–I(3)	102.52(10)
I(3)#4–Ag(3)–I(2)#3	103.72(10)	I(2)–Ag(3)–I(2)#3	106.17(10)	I(3)#1–Ag(2)–Ag(3)#1	58.00(8)	I(2)#3–Ag(3)–Ag(2)	130.65(13)
I(3)#4–Ag(3)–Ag(2)	125.29(13)	I(2)–Ag(3)–I(3)	113.87(10)	I(3)#4–Ag(3)–I(2)	116.53(11)	I(3)#4–Ag(3)–Ag(2)#3	112.97(12)
I(3)–Ag(3)–Ag(2)#3	54.78(9)	I(3)–Ag(3)–Ag(2)	54.53(9)	I(2)–Ag(3)–Ag(2)#3	130.47(14)	I(2)#3–Ag(3)–Ag(2)#3	59.09(9)

[a] Symmetry transformations used to generate equivalent atoms: #1: x, $y + 1$, z; #2: $-x + 1/2$, $y + 1/2$, $-z + 1/2$; #3: x, $y - 1$, z; #4: $-x + 1/2$, $-y - 1/2$, $-z + 1$; #5: $-x + 1/2$, $y - 1/2$, $-z + 1/2$; #6: $-x$, y, $-z + 1/2$.

Table 3. Selected bond lengths [Å] and angles [°] for **3** and **4**.[a]

Compound **3**							
Pb(1)–N(2)#1	2.64(3)	Pb(1)–I(1)	3.154(2)	Pb(1)–I(2)#2	3.165(2)	Pb(1)–I(2)	3.280(2)
Pb(1)–I(1)#3	3.315(2)	I(1)–Pb(1)#2	3.315(2)	I(2)–Pb(1)#3	3.165(2)	N(2)–Pb(1)#4	2.64(3)
N(2)#1–Pb(1)–I(1)	98.0(7)	N(2)#1–Pb(1)–I(2)#2	91.7(6)	I(1)–Pb(1)–I(2)#2	93.06(5)	N(2)#1–Pb(1)–I(2)	81.5(7)
I(1)–Pb(1)–I(2)	177.27(5)	I(2)#2–Pb(1)–I(2)	89.63(5)	N(2)#1–Pb(1)–I(1)#3	87.6(6)	I(1)–Pb(1)–I(1)#3	89.18(5)
I(2)#2–Pb(1)–I(1)#3	177.71(6)	I(2)–Pb(1)–I(1)#3	88.12(5)	Pb(1)–I(1)–Pb(1)#2	89.18(5)	Pb(1)#3–I(2)–Pb(1)	89.63(5)
Compound **4**							
I(1)–I(3)	2.9012(10)	I(1)–I(2)	2.9204(10)	N(1)–C(1)	1.333(10)	N(1)–C(5)	1.343(9)
N(2)–C(13)	1.338(9)	N(2)–C(9)	1.342(9)				
I(3)–I(1)–I(2)	178.11(3)	C(1)–N(1)–C(5)	118.2(7)	C(13)–N(2)–C(9)	119.9(7)	N(1)–C(1)–C(2)	122.2(8)
C(4)–C(3)–C(2)	116.9(7)	N(1)–C(5)–C(4)	122.5(7)	C(3)–C(6)–C(7)	108.6(6)	C(6)–C(7)–C(8)	113.7(6)
C(11)–C(8)–C(7)	109.3(6)	C(12)–C(11)–C(10)	117.0(6)				

[a] Symmetry transformations used to generate equivalent atoms in **3**: #1: x, $y - 1$, z; #2: $x + 1$, y, z; #3: $x - 1$, y, z; #4: x, $y + 1$, z.

Table 4. Crystal data, data collection, and structure-refinement parameters for **1**–**4**.

Compound	$[(CuI)_4(bpp)_4]_n$ (**1**)	$[(AgI)_6(bpp)]_n$ (**2**)	$[PbI_2(bpp)]_n$ (**3**)	$[I_3(bppH)]$ (**4**)
Formula	$C_{52}H_{56}Cu_4I_4N_8$	$C_{13}H_{14}Ag_6I_6N_2$	$C_{13}H_{14}I_2N_2Pb$	$C_{13}H_{15}I_3N_2$
Formula weight	1554.81	1606.88	659.25	579.97
Crystal system	tetragonal	monoclinic	monoclinic	orthorhombic
Space group	$P4_12_12$	$C2/c$	$P2_1$	$Pbca$
a [Å]	12.5555(2)	29.891(6)	4.5429(9)	17.245(3)
b [Å]	12.5555(2)	4.5617(9)	15.305(3)	9.4476(19)
c [Å]	36.437(7)	23.470(5)	11.925(2)	21.811(4)
β [°]	90	123.37(3)	95.00(3)	90
Volume [Å^3]	5743.9(16)	2672.7(9)	825.9(3)	3553.5(12)
Z	4	4	2	8
$\rho_{calcd.}$ [Mg m^{-3}]	1.798	3.993	2.651	2.168
μ [mm^{-1}]	3.651	11.245	13.937	5.265
$F(000)$	3008	2824	588	2128
Temperature [K]	291(2)	291(2)	291(2)	291(2)
λ (Mo-K_α) [Å]	0.71073	0.71073	0.71073	0.71073
Reflections collected	10600	3371	2130	8775
Independent reflections	10284	2046	1994	2977
Goodness-of-fit on F^2	1.027	1.137	1.075	1.137
Final R_1,[a] wR_2[b]	0.0448, 0.0741	0.0870,0.2626	0.0951, 0.2475	0.0514, 0.1060
R indices (all data)	0.1074, 0.0862	0.1030, 0.2813	0.0951, 0.2475	0.0845, 0.1172
Largest peak, hole [e Å^{-3}]	0.002, 0.000	2.318, –3.230	6.436, –2.119	0.990, –0.973

[a] $R_1 = \Sigma||F_o| - |F_c||/\Sigma|F_o|$. [b] $wR_2 = [\Sigma w(|F_o^2| - |F_c^2|)^2/\Sigma w|F_o^2|^2]^{1/2}$. $w = 1/[\sigma^2(F_o)^2 + 0.0297P^2 + 27.5680P]$, where $P = (F_o^2 + 2F_c^2)/3$.

4.75. IR (KBr): $\tilde{\nu}$ = 3029 (w), 2922 (w), 1616 (s), 1501 (w), 1406 (w), 1351 (w), 1223 (w), 1029 (m), 816 (m), 618 (w), 552 (w), 442 (w) cm^{-1}.

Nonlinear Optical Measurements: The optical measurements were performed with linearly polarized 8-ns pulses at 532 nm generated from a frequency-doubled Q-switched Nd:YAG laser. This wavelength is of paramount practical importance in the field of optical limiting as well as the design and fabrication of resonance cavities of lasers. The spatial profiles of the pulses were nearly Gaussian after a spatial filter was employed. A DMF solution of compound **1** was placed in a 1-mm-thick quartz cell for optical limiting measurements. Crystalline samples of **1** are stable toward oxygen, moisture, and laser light. The laser pulse was focused into the cells containing the non-linear medium with a 250-mm focal length lens. The laser beam was divided into two beams. One was used to monitor the incident laser energy meter and the other was focused onto the sample cell. The input and the output energies of the beams were measured with an energy meter (Laser Precision Rjp-735), which were linked to a computer by an IEEE interface.[30,31] The experimental data were collected utilizing a single shot at a rate of 1 pulse per minute to avoid the influence of thermal effects.

X-ray Crystallography: Crystallographic data for the title compounds were collected using Mo-K_α radiation (λ = 0.71073 Å) on a Rigaku RAXIS-IV image plate area detector. The data were corrected for Lorentz and polarization factors and for absorption by using empirical scan data. The structure was solved with the SHELX program,[32] and refined by full-matrix least-squares methods based on F^2, with anisotropic thermal parameters for the non-hydrogen atoms. The hydrogen atoms were located theoretically and not refined. Selected bond lengths and bond angles for **1** (Table 1), **2** (Table 2), and **3** and **4** (Table 3) are given below. Crystal data are summarized in detail in Table 4.

CCDC-252911 (for **1**), -287706 (for **2**), -287707 (for **3**), and -287708 (for **4**) contain the supplementary crystallographic data for this paper. These data can be obtained free of charge from The Cambridge Crystallographic Data Center via www.ccdc.cam.ac.uk/data_request/cif.

Acknowledgments

This research was funded by the National Natural Science Foundation (grant no. 20371042), the Henan Province Excellent Young Foundation (grant no. 2005002800), and the China Postdoctoral Science Foundation (2003033525). The author also thanks one of the referees, Prof. Richard E. Marsh, and Guang Yang for their helpful comments.

[1] a) J. M. Lehn, *Supramolecular Chemistry: Concepts and Perspectives*, VCH, Weinheim, **1995**, p. 89; b) A. J. Blake, N. R. Champness, P. Hubberstey, W. S. Li, M. A. Withersby, M. Schroder, *Coord. Chem. Rev.* **1999**, *183*, 117–138; c) S. Kitagawa, R. Kitaura, S. I. Noro, *Angew. Chem. Int. Ed.* **2004**, *43*, 2334–2375.
[2] M. Fujita, Y. J. Kwon, S. Washizu, K. Ogura, *J. Am. Chem. Soc.* **1994**, *116*, 1151–1152.
[3] O. R. Evans, W. Lin, *Acc. Chem. Res.* **2002**, *35*, 511–522.
[4] O. Kahn, *Acc. Chem. Res.* **2000**, *33*, 647–657.
[5] a) B. F. Hoskins, R. Robson, D. A. Slizys, *J. Am. Chem. Soc.* **1991**, *119*, 2952–2953; b) S. R. Batten, R. Robson, *Angew. Chem. Int. Ed.* **1998**, *37*, 1460–1494; c) L. Carlucci, G. Ciani, D. M. Proserpio, *Coord. Chem. Rev.* **2003**, *246*, 247–289.
[6] a) S. L. Price, A. J. Stone, J. Lucas, R. S. Rowland, A. E. Thornley, *J. Am. Chem. Soc.* **1994**, *116*, 4910–4918; b) G. R. Desiraju, *Angew. Chem. Int. Ed. Engl.* **1995**, *34*, 2311–2327.
[7] a) C. Hamers, O. Kocian, F. M. Raymo, J. F. Stoddart, *Adv. Mater.* **1998**, *10*, 1366–1369; b) F. M. Raymo, J. F. Stoddart, *Chem. Rev.* **1999**, *99*, 1643–1664; c) H. F. Zhu, J. Fan, T. A. Okamura, W. Y. Sun, N. Ueyama, *Cryst. Growth Des.* **2005**, *5*, 289–294.
[8] M. Fujita, *Acc. Chem. Res.* **1999**, *32*, 53–61.
[9] a) P. H. Svensson, L. Kloo, *Chem. Rev.* **2003**, *103*, 1649–1684; b) L. M. Castro-Castro, M. G. Arnold, *Inorg. Chem.* **2004**, *43*, 4537–4539.
[10] Y. Y. Niu, H. W. Hou, Y. Zhu, *J. Cluster Sci.* **2003**, *14*, 483–493.
[11] Y. Y. Niu, Y. L. Song, H. W. Hou, Y. Zhu, *Inorg. Chem.* **2005**, *44*, 2553–2559.
[12] a) M. J. Plater, M. R. S. J. Foreman, T. Gelbrich, S. J. Coles, M. B. Hursthouse, *J. Chem. Soc., Dalton Trans.* **2000**, 3065–3073; b) S. A. Barnett, N. R. Champness, *Coord. Chem. Rev.* **2003**, *246*, 145–168; c) A. Erxleben, *Coord. Chem. Rev.* **2003**, *246*, 203–228; d) K. Jin, X. Huang, L. Pang, J. Li, A. Appel, S. Wherland, *Chem. Commun.* **2002**, 2872–2873; e) L. Carlucci, G. Ciani, M. Moret, D. M. Proserpio, S. Rizzato, *Chem. Mater.* **2002**, *14*, 12–16.
[13] a) H. W. Hou, Y. L. Song, H. Xu, Y. Wei, Y. T. Fan, Y. Zhu, L. Li, C. Du, *Macromolecules* **2003**, *36*, 999–1008; b) Y. Y. Niu, Y. L. Song, J. Wu, H. W. Hou, Y. Zhu, *Inorg. Chem. Commun.* **2004**, *7*, 471–474; c) Y. Y. Niu, Y. L. Song, H. W. Hou, Y. Zhu, *Inorg. Chim. Acta* **2003**, *355*, 151–156.
[14] Y. Y. Niu, H. G. Zheng, H. W. Hou, X. Q. Xin, *Coord. Chem. Rev.* **2004**, *248*, 169–183.
[15] a) S. Myllyviita, R. Sillanpaa, *J. Chem. Soc., Dalton Trans.* **1994**, 2125–2128; b) B. Corradi, M. R. Cramarossa, T. Manfredini, L. P. Battaglia, G. Pelosi, A. Saccani, F. Sandrolini, *J. Chem. Soc., Dalton Trans.* **1993**, 3587–3591; c) G. Helgesson, S. Jagner, *J. Chem. Soc., Dalton Trans.* **1990**, 2413; d) M. A. S. Goher, A. K. Hafez, T. C. W. Mak, *Polyhedron* **2001**, *20*, 2583–2587.
[16] a) K. R. Kyle, C. K. Ryu, J. A. DiBenedetto, P. C. Ford, *J. Am. Chem. Soc.* **1991**, *113*, 2954–2965; b) M. Vitale, P. C. Ford, *Coord. Chem. Rev.* **2001**, *219–221*, 3–16; c) A. Pfitzner, S. Reiser, H. J. Deiseroth, *Z. Anorg. Allg. Chem.* **1999**, *625*, 2196–2201; d) C. M. Fitchett, P. J. Steel, *New J. Chem.* **2000**, *24*, 945–947; e) L. R. Hanton, K. Lee, *J. Chem. Soc., Dalton Trans.* **2000**, 1161–1166; f) X. Y. Liu, *Chem. Commun.* **1998**, 1149–1150; g) I. M. Müller, T. Röttgers, W. S. Sheldrick, *Chem. Commun.* **1998**, 823–824; h) N. R. Brooks, A. J. Blake, N. R. Champness, P. A. Cooke, P. Hubberstey, D. M. Proserpio, C. Wilson, M. Schröder, *J. Chem. Soc., Dalton Trans.* **2001**, 456–465; i) S. R. Batten, J. C. Jeffery, M. D. Ward, *Inorg. Chim. Acta* **1999**, *292*, 231; j) S. Hu, M. L. Tong, *Dalton Trans.* **2005**, 1165–1167.
[17] a) G. Helgesson, S. Jagner, *J. Chem. Soc., Dalton Trans.* **1990**, 2413–2420; b) A. J. Blake, N. R. Brooks, N. R. Champness, P. A. Cooke, A. M. Deveson, D. Fenske, P. Hubberstey, W. S. Li, M. Schröder, *J. Chem. Soc., Dalton Trans.* **1999**, 2103–2110; c) Q. X. Liu, F. B. Xu, Q. S. Li, X. S. Zeng, X. B. Leng, Y. L. Chou, Z. Z. Zhang, *Organometallics* **2003**, *22*, 309–314; d) M. Massaux, M. T. L. Bihan, R. Chevalier, *Acta Crystallogr., Sect. B* **1977**, *33*, 2084–2091.
[18] a) Y. J. Shi, Y. Xu, Y. Zhang, B. Huang, D. R. Zhu, C. M. Jin, H. G. Zhu, Z. Yu, X. T. Chen, X. Z. You, *Chem. Lett.* **2001**, 678–679; b) Y. J. Shi, L. H. Li, Y. Z. Li, Y. Xu, X. T. Chen, Z. L. Xue, X. Z. You, *Inorg. Chem. Commun.* **2002**, *5*, 1090–1094; c) L. Y. Kong, Z. H. Zhang, T. Okamura, M. J. Fei, W. Y. Sun, N. Ueyama, *Chem. Lett.* **2004**, *33*, 1572–1573.
[19] J. I. Jay, C. W. Padgett, R. D. B. Walsh, T. W. Hanks, W. T. Pennington, *Crystal Growth Des.* **2001**, *1*, 501–507.
[20] V. W. W. Yam, K. K. W. Lo, *Chem. Soc. Rev.* **1999**, *28*, 323–334.
[21] X. H. Bu, H. Liu, M. Du, K. M. C. Wong, V. W. W. Yam, *Inorg. Chim. Acta* **2002**, *333*, 32–40.
[22] J. L. Bredas, C. Adant, P. Tackx, A. Persoons, *Chem. Rev.* **1994**, *94*, 243–278.

[23] Z. Burshtein, Y. Kostoulas, H. M. Van, *J. Opt. Soc. Am. B* **1997**, *14*, 2477–2487.
[24] P. Ge, S. H. Tang, W. Ji, S. Shi, H. W. Hou, D. L. Long, X. Q. Xin, S. F. Lu, Q. J. Wu, *J. Phys. Chem. B* **1997**, *101*, 27–31.
[25] G. Sakane, T. Shibahare, H. W. Hou, X. Q. Xin, S. Shi, *Inorg. Chem.* **1995**, *34*, 4785–4789.
[26] H. W. Hou, Y. T. Fan, C. X. Du, Y. Zhu, W. L. Wang, X. Q. Xin, M. K. M. Low, W. Ji, H. G. Ang, *Chem. Commun.* **1999**, 647–648.
[27] S. Shi, W. Ji, S. H. Tang, J. P. Lang, X. Q. Xin, *J. Am. Chem. Soc.* **1994**, *116*, 3615–3616.
[28] Y. P. Sun, J. E. Riggs, *Int. Rev. Phys. Chem.* **1999**, *18*, 43–90.
[29] H. W. Hou, Y. L. Wei, Y. L. Song, L. W. Mi, M. S. Tang, L. K. Li, Y. T. Fan, *Angew. Chem. Int. Ed.* **2005**, *44*, 6067–6074.
[30] M. Sheik-Bahae, A. A. Said, T. H. Wei, D. J. Hangan, E. W. Van Stryland, *IEEE J. Sel. Top. Quantum Electron.* **1990**, *26*, 760–769.
[31] M. Sheik-Bahae, A. A. Said, E. W. Van Stryland, *Opt. Lett.* **1989**, *14*, 955–957.
[32] G. M. Sheldrick, SHELXTL-93, University of Göttingen, Germany, **1993**.

Received: October 27, 2005
Published Online: March 31, 2006

